School of Mathematics, Meteorology
and Physics

University of Reading

Department of Mathematics

Preprint MPS_2009-15

2 October 2009

The flow induced dynamic surface tension effects at nanoscale

by

A.V. Lukyanov

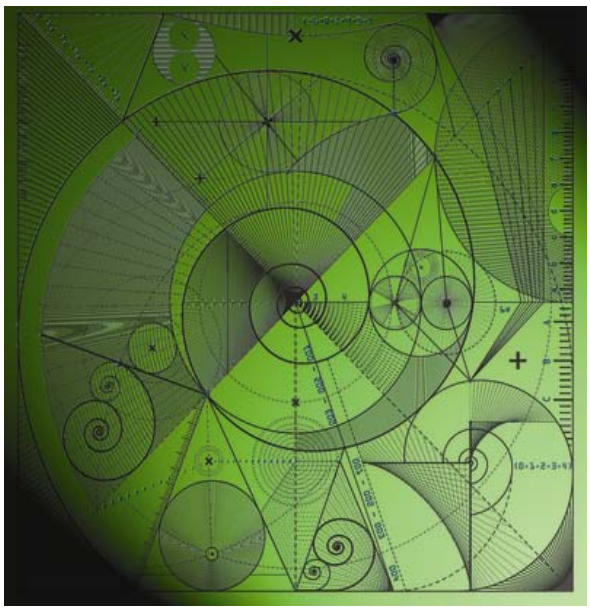

The flow induced dynamic surface tension effects at nanoscale.

A. V. Lukyanov

Department of Mathematics, University of Reading, Reading RG6 6AX, U.K.

Abstract

The aim of this report is to describe the effects of dynamic surface tension solely induced by the nanoscale topography of the substrates. The flow induced surface tension effects are examined on the basis of a sharp interface model. It is demonstrated how nanoscale objects placed at the boundary of the flow domain result in generation of substantial surface forces acting on the bulk flow.

The distinctive feature of fluid motion at nanoscale is its strong coupling with the dynamic processes in the interfacial layers formed at the boundaries between the phases[1−2]. For example, we know from recent experiments that slippage of liquids at solid substrates results in enhanced liquid transport through nanoscale capillary channels, up to 45-400 times higher in comparison to the theoretical predictions based on the no-slip boundary condition[3−4]. The slippage of liquids is only one manifestation of interfacial dynamic properties. Another effect associated with the formation of interfacial layers and widely exploited to control nanoflows is surface tension[5−7].

If a moving contact line is present, the dynamic surface tension effects manifest themselves in the dependence of the contact angle $\theta_d(u_c)$ formed between the moving free surface and the solid substrate on the velocity of the triple-phase contact line, u_c[6−8]. This can be illustrated by the Young equation, $\cos\theta_d\sigma_{GL} = -\sigma_{LS}+\sigma_{GS}$, where σ_{GL}, σ_{LS}, σ_{GS} are the surface tensions of gas-liquid, liquid-solid and gas-solid interfaces, evaluated at the contact line. The dependence $\theta_d(u_c)$ implies that at least some of the surface tensions are not equal to their equilibrium values when the contact line is at rest. The velocity-dependence of the dynamic contact angle is only one part of its general dependence; apart from the substrate velocity, the contact angle is a functional of the entire flow field at the contact line region. This effect is known as the non-locality of dynamic contact angle or, in macroscopic context, as the hydrodynamic assist of dynamic wetting, which has been used for decades in the coating industries[9].

Studies of the effects of dynamic wetting on smooth flat surfaces (in particular the effect of non-locality) have revealed several characteristic features of the interfacial phase dynamics. That is that slippage of liquids and the dynamic surface tensions are closely interrelated, the σ_{GL}, σ_{LS} surface tensions at the contact line deviate from the equilibrium values and equilibrate over the distance, away from the contact line region, defined by the characteristic diffusion time in the interfacial layer, that is by the characteristic time of the formation of the interfacial layers[7,9−15]. This scenario has been further supported by the evidence from independent studies of viscous flows over the surfaces with variable wettability, where the changes of the liquid-solid interfacial energy $\sigma_{LS}(x)$ have been achieved by chemical patterning of the substrate[16−17].

In this letter, we investigate the effect, especially relevant to nanofluidic flows, of coupling of the surface topography and the flow induced surface tensions. The question is, what if we change the flat geometry of the solid surface by placing a tiny, nanoscale obstacle on the surface? The effect from a particle arrested on a substrate is well studied for macroscopic incompressible flows[18−19]. But, if the obstacle is of the size of the interfacial layer, where incompressibility condition is relaxed to account for surface tension, then one would expect to observe completely new effects since the presence of an obstacle may disturb the surface phase density equilibrium state and cause variations in the surface tension, similar to the Marangoni effect, though in this case solely induced by the surface topography.

The analysis of this problem is based on the sharp

interface formation theory[7], given the length scale of the interfacial region of a few nanometres[20], coupled with the effect of surface slip[21−22]. This approach, first developed using methods of non-equilibrium thermodynamics[23], is based on the standard set of the Navier-Stokes equations, taken in the context of nanoflows with negligible inertia, for the flow velocity $\mathbf{u}$ and pressure p in the bulk of an incompressible and, for simplicity, Newtonian liquid with viscosity μ and density ρ,

$$\nabla \cdot \mathbf{u} = 0, \quad \nabla p = \mu \nabla^2 \mathbf{u}, \tag{1}$$

and an extended set of boundary conditions[7], at the solid substrate, at $y = 0$, which describes a coupling between the bulk phase, the surface phase in the interfacial layer and the solid substrate, Fig.1. In the sharp interface limit, the thickness of the interfacial layer is zero, and the surface phase is solely characterised by two-dimensional distributions of the surface velocity $\mathbf{v^s}$ and surface density ρ^s, which are integrated values over the interfacial layer. The solid substrate is impermeable, so,

$$\mathbf{v}^s \cdot \mathbf{n} = 0, \tag{2}$$

where $\mathbf{n}$ is the normal vector at the substrate pointing into the liquid. The second boundary condition is the tangential stress balance equation in the interfacial layer, which is, in fact, a modified Navier condition[7], with the coefficient of surface slip β_s[21−22]. This condition also takes into account the Marangoni effect where the flow is driven by the surface-tension gradient $\nabla\sigma$ and thus links the effects of slip and surface tension[7,17],

$$\mu \mathbf{n} \cdot [\nabla \mathbf{u} + (\nabla \mathbf{u})^*] \cdot (\mathbf{I} - \mathbf{nn}) + \nabla \sigma = \beta_s \mathbf{u} \cdot (\mathbf{I} - \mathbf{nn}), \tag{3}$$

here $\mathbf{I}$ is the metric tensor; the tensor $(\mathbf{I} - \mathbf{nn})$ singles out the tangential projection of a vector; an asterisk marking a second-rank tensor indicates its transposition. Note, that we have neglected the effect of apparent slip, the full analysis can be found elsewhere[24], so the tangential component of the velocity $\mathbf{u}$ on the *liquid*-facing side of the interface, Fig.1, is simply equal to the surface phase velocity,

$$\mathbf{v^s} = \mathbf{u}. \tag{4}$$

The set of boundary conditions is completed by two equations describing the mass exchange between the bulk and the surface phase that takes place when the surface density ρ^s deviates from its equilibrium value ρ^s_e,

$$\rho \mathbf{u} \cdot \mathbf{n} = (\rho^s - \rho^s_e)\tau^{-1}, \tag{5}$$

$$\frac{\partial \rho^s}{\partial t} + \nabla \cdot (\rho^s \mathbf{v}^s) = -(\rho^s - \rho^s_e)\tau^{-1}, \tag{6}$$

and an equation of state relating the surface tension and the surface density, which is taken for simplicity in a linear form,

$$\sigma = \gamma(\rho^s_0 - \rho^s), \tag{7}$$

here parameter τ is the surface density relaxation time, ρ^s_0 is the characteristic surface density when the surface tension is zero and γ is a phenomenological material constant.

We consider a steady-state solution to (1)–(7), assuming that the obstacle blocks the flux in the interfacial layer, that is at the boundary Γ of the obstacle,

$$\mathbf{v^s} \cdot \mathbf{n_s}|_\Gamma = 0, \tag{8}$$

and the flow is driven by a plane-parallel constant shear $\mathbf{S_0}$ in the far field, which is directed, without loss of generality, along the x-axis, Fig.1. Here, $\mathbf{n_s}$ is the external normal vector in the substrate plane to the boundary $\Gamma(x, z) = 0$.

Two-dimensional analysis of the problem, in the (x, y) plane, in the case of a lattice of one-dimensional nanothreads lying on the solid substrate normal to the flow, has been done previously[24]. It has been shown that, if we use $L = \lambda = \mu/\beta_s$, $U_0 = LS_0$, $p_0 = \frac{\mu U_0}{L}$ and ρ^s_e as scales for velocity, length, pressure and the surface density; λ is the characteristic slip length, then the problem has three non-dimensional parameters $\epsilon = \frac{U_0\tau}{\lambda}$, $Ca = \frac{\mu U_0}{\sigma_0}$, $Q = \frac{\rho^s_e}{\rho\lambda}$; parameter $\sigma_0 = \gamma\rho^s_e$ is the characteristic surface tension, γ is inversely proportional to the fluid's compressibility and is, roughly, the square of the speed of sound; $\rho^s_e \sim \rho^s_0 \sim \rho h$, h is the interfacial thickness. Parameter ϵ is the ratio of the characteristic relaxation length $U_0\tau$ to the characteristic slip length λ, Ca is the capillary number, parameter $Q \simeq h/\lambda$ characterizes the mass flux into/out of the liquid-solid interface. It is usual that $Ca << 1$ and $Q << 1$, and it is common that $\epsilon << 1$, while the ratio $Ca/\epsilon = \xi_0^2 \sim O(1)$, see estimates[24]. Under those

conditions, an asymptotic analysis of the above simplified two-dimensional problem has shown that substantial perturbations of the surface tension, sufficient to affect flow conditions at the substrate, exist over the distance $l_0 = \sqrt{\lambda\tau\sigma_0/\mu}$ defined by the surface phase relaxation time [24].

Now, we consider a general case of two-dimensional nanoparticles of an arbitrary shape with a smooth boundary $\Gamma_k(x,z) = 0$ of the domain Ω_k occupied by the nanoparticle on the (x,z) plane. One can show that, in the same limit[24], the problem (1)–(7) can be reduced to an exterior Neumann boundary value problem for the modified Helmholtz equation on an unbounded domain, which is in the non-dimensional form,

$$\Delta\rho_1^s - \xi_0^2\rho_1^s = 0, \quad \mathbf{x} \in \mathbb{R}^2 \setminus \bigcup_k \bar{\Omega}_k \tag{9}$$

$$\lim_{r\to\infty} \rho_1 = 0, \quad |\mathbf{x}| = r,$$

$$\rho^s = 1 + \epsilon\rho_1^s,$$

with the boundary condition (8), on $\Gamma = \bigcup_k \Gamma_k$ in the form

$$\left.\frac{\partial\rho_1^s}{\partial n_s}\right|_\Gamma = \xi_0^2 \mathbf{n_s}\cdot\frac{\mathbf{S_0}}{S_0}, \quad \xi_0^2 = \frac{Ca}{\epsilon} = \frac{\lambda^2}{l_0^2}. \tag{10}$$

To arrive at (9), it is sufficient to assume that the shear rate $\mathbf{S} = \partial\mathbf{u}_\parallel/\partial n$ has the same constant value, $\mathbf{S_0}$, up to the *liquid*-facing side of the interfacial layer - this is the case, for example, if the length scale of the perturbation region is much larger than λ (in the case of nanothreads, if $\xi_0 << 1$).

The velocity component at the *liquid*-facing side of the interfacial layer can be expressed through ρ_1^s as,

$$\mathbf{u}\cdot(\mathbf{I} - \mathbf{nn}) = \frac{\mathbf{S_0}}{S_0} - \xi_0^{-2}\nabla\rho_1^s, \tag{11}$$

so that even small perturbations of the surface density ($\sim \epsilon$) will have strong effect on the flow conditions at the substrate.

In general, a solution to (9)–(10) can be obtained numerically using a boundary integral method[28], which has superalgebraic or even exponential rate of convergence. This technique is especially advantageous if one has to deal with many particles distributed on the surface and is the basis for simulations in this study.

But, first, we consider just one circular obstacle of radius R_0 when a general analytical solution to (9)–(10) is available, which is, in a polar coordinate system with the origin at the centre of the obstacle, Fig.1,

$$\begin{gathered}\rho^s(r,\phi) = 1 + \epsilon A\cos(\phi)K_1(\xi_0 r),\\ \sigma(r,\phi) = \tfrac{\rho_0^s}{\rho_e^s} - \rho^s,\\ A = -\xi_0(K_0(\xi_0 R_0) + K_1(\xi_0 R_0)/\xi_0 R_0)^{-1},\end{gathered} \tag{12}$$

here, $K_0(z)$ and $K_1(z)$ are the modified Bessel functions of the second kind. If $\xi_0 << 1$,

$$\rho^s(r,\phi) \simeq 1 - Ca\, R_0\,\frac{R_0}{r}\cos(\phi), \tag{13}$$

$$\sigma \simeq \frac{\rho_0^s}{\rho_e^s} - 1 + Ca\, R_0\,\frac{R_0}{r}\cos(\phi). \tag{14}$$

From this simple analytical result, one can learn that, in general, the surface phase is compressed at the *flow*-facing side of the obstacle and is rarefied in the wake, and, for a circular-like object, (a) the topography induced surface tension perturbations vanish with the size of the obstacle R_0, (b) the perturbation region is defined by the size of nanoparticles R_0 in contrast to the case of nanothreads[24], where the characteristic distance is defined by the surface phase relaxation process (by the parameter ξ_0), (c) the strength of the effect is simply defined by the capillary number Ca, that is by the applied shear rate and the slip length, in contrast to the case of nanothreads[24], where the effect is proportional to Ca/ξ_0.

Consider for illustration a particular example of a viscous liquid from the range of PDMS fluids with $\mu = 1$ Pa s and $\sigma_{GL} = 2\times10^{-2}$ N/m at characteristic shear rate $S_0 \sim 10^4$ s^{-1}, when the liquid is still Newtonian. The characteristic slip length may be chosen in the range observed for this kind of fluids $\lambda \sim 100$ nm[25]. The parameters τ and $\frac{\rho_0^s}{\rho_e^s}$ (to calculate surface tension) are taken to scale, according to the estimates obtained from experiments on dynamic wetting[26], as $\tau = 10^{-8}\left(\frac{\mu}{1\ mPa\ s}\right)\ s$, $\frac{\rho_0^s}{\rho_e^s} \simeq (1 + 0.3\cos(\theta_0))^{-1}$ for a liquid-solid combination with the static contact angle θ_0. At $\theta_0 = 60°$, parameters $\sigma_0 \simeq 7\times10^{-2}$ N/m, $\epsilon \sim 0.1$ and $Ca \sim 10^{-2}$, resulting in variations of the surface tension $\Delta\sigma/\sigma \sim 0.1$ at $R_0 = 1$. Obviously, at higher viscosities, for larger obstacles, $R_0 > 1$, and at static contact angles closer to $\theta_0 = 90°$, the effect is much stronger, $\Delta\sigma/\sigma \sim 1$. The distribution of the generated surface tensions is illustrated in Fig.2.

Now, we will look at the effect of the obstacle shape by considering single, but extended structures. One might expect to have similar, to the case of nanothreads[24], parametric dependence , when the perturbation region is defined by the parameter ξ_0. In simulations, we kept $Ca = const$, but vary ξ_0. If the effect would be similar to the one observed for circular obstacles, then we would not see any clear dependence on ξ_0. On the other hand, if the effect is similar to the one observed for nanothreads[24], then we should observe such dependence. The results are shown in Fig.3 for different values of ξ_0. One can clearly see that the perturbation zone and the amplitude increase as ξ_0 decreases. But, note, that the effect saturates at ξ_0^{-1} much larger than the maximal dimension of the obstacle.

Finally, we consider the effect of clustered circular nanoobstacles. The results of simulations are presented in Fig.4. While one can see some collective effects induced by the obstacles, the phenomenon is largely similar to the one observed for a single circular obstacle.

In conclusion, it has been shown that nanoscale topography of the substrate is a signifacant factor, which results in generation of noticeable surface tension stresses, which can not be ignored in simulations of flows at nanoscale. The generated surface tensions have the most effect on the velocity field at the substrate and in the case of asymmetric extended structures or nanothreads. Remarkably, the effect on the velocity field is independent of the applied shear rate, but the domain grows, in general, as $\sqrt{\lambda}$, (11).

Acknowledgment

The author is very grateful to S.Langdon for his help with numerical simulations.

---

[1] Zhao, B., Moore, J.S., Beebe, D.J., (2002) Anal. Chem. 74 4259–4268.

[2] Squires, T.M. and Quake, S.R., (2005) Rev. Mod. Phys. 77 977–1026.

[3] Whitby, M., Cagnon, L., Thanou, M., Quirke, N., (2008) Nano letters 8 2632–2637.

[4] Thomas, J.A., McGaughey, A.J.H., (2008) Nano letters 8 2788–2793.

[5] Darhuber, A.A., Troian, S.M., (2005) Annu. Rev. Fluid Mech. 37 425–455..

[6] Blake, T.D., (2006) J. Colloid Interface Sci. 299 1–13.

[7] Shikhmurzaev, Y.D., (2007) *Capillary Flows with Forming Interfaces.* Taylor & Francis.

[8] Ralston, J., Popescu, M., Sedev, R. , (2008) Annu. Rev. Mater. Res. 38 23–43.

[9] Blake, T.D., Clarke, A., Rushak, K.J., (1994) AIChE J. 40 229–242.

[10] Blake, T.D., Bracke M, Shikhmurzaev, Y.D. , (1999) Phys. Fluids 11 1995–2007.

[11] Bayer, I.S., Megaridis, C.M., (2006) J. Fluid Mech. 558 415–449.

[12] Clarke, A., Stattersfield, E., (2006) Phys. Fluids 18 048106.

[13] Lukyanov, A., Shikhmurzaev, Y.D., (2006) Phys. Lett. A 358 426–430.

[14] Yamamura, M., (2007) Colloid. Surface. A 311 55–60.

[15] Lukyanov, A., Shikhmurzaev, Y.D., (2007) Phys. Rev. E 75 051604.

[16] Priezjev, N.V., Darhuber, A.A., Troian, S.M., (2005) Phys. Rev. E 71 041608.

[17] Sprittles, J.E., Shikhmurzaev, Y.D., (2007) Phys. Rev. E 76 021602.

[18] Pozrikidis, C., Thoroddsen, S.T., (1991) Phys. Fluids A 3 2546-2558.

[19] Blyth, M.G., Pozrikidis, C., (2006) Phys. Fluids 18 052104.

[20] Derjaguin, B.V., Churaev, N.V., Muller, V.M. , (1987) *Surface forces* New York: Consultants. Bureau.

[21] Bocquet. L., Barrat, J.L., (1994) Phys. Rev. E 49 3079–3092.

[22] Barrat, J.L., Bocquet. L., (1999) Phys. Rev. Lett. 82 4671–4674.

[23] Bedeaux, D., Albano, A.M., Mazur, P., (1975) Physica A 82 438–462..

[24] Lukyanov, A., (2009) Phys. Lett. A 373 1967–1971.

[25] Hervet, H., Leger, L., (2003) Comptes Rendus Physique 4 241–249.

[26] Blake, T. D. and Shikhmurzaev, Y. D., (2002) J. Colloid Interface Sci. 253 196–202.

[28] Langdon, S., Graham, I.G., (2001) IMA journal of Numerical Analysis 21 217-237.

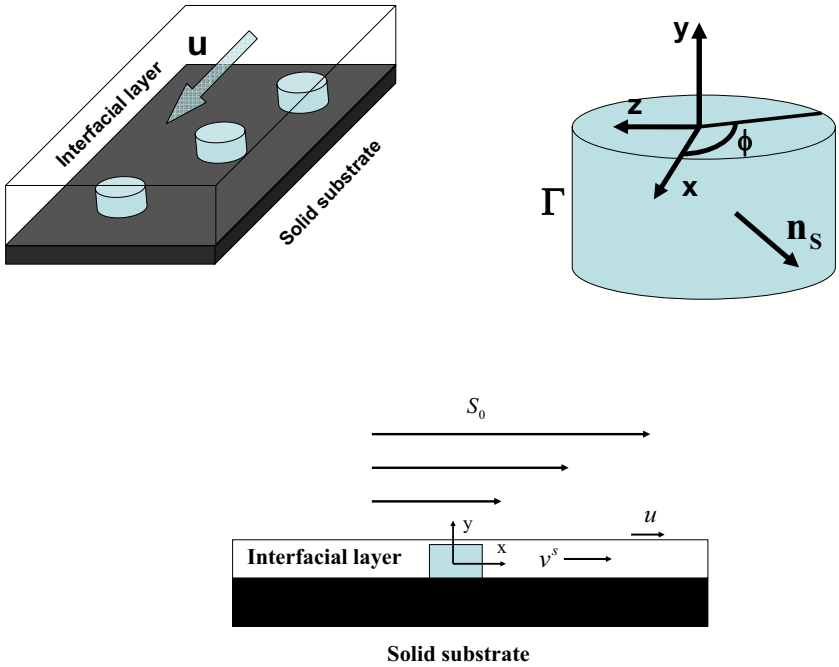

Figure 1: Definition sketch for the problem.

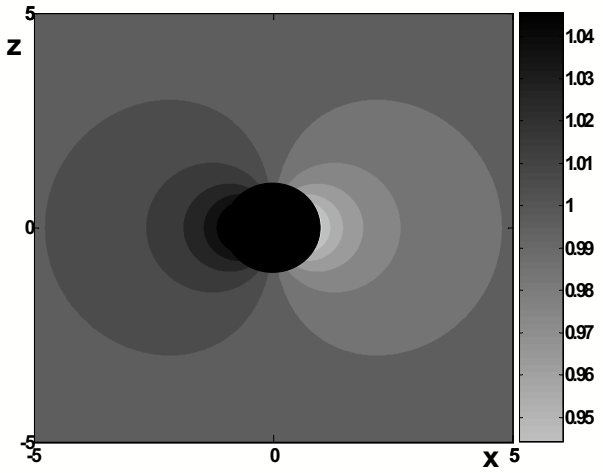

Figure 2: The distribution of the surface tension induced by a circular obstacle at $R_0 = 1$, $\theta_0 = 60°$, $\epsilon = 0.1$ and $Ca = 0.01$. The surface tension is normalised by its value in the far field σ_∞ at $r \to \infty$ and the length is normalised by the slip length λ. The dark black area corresponds to the area occupied by the obstacle.

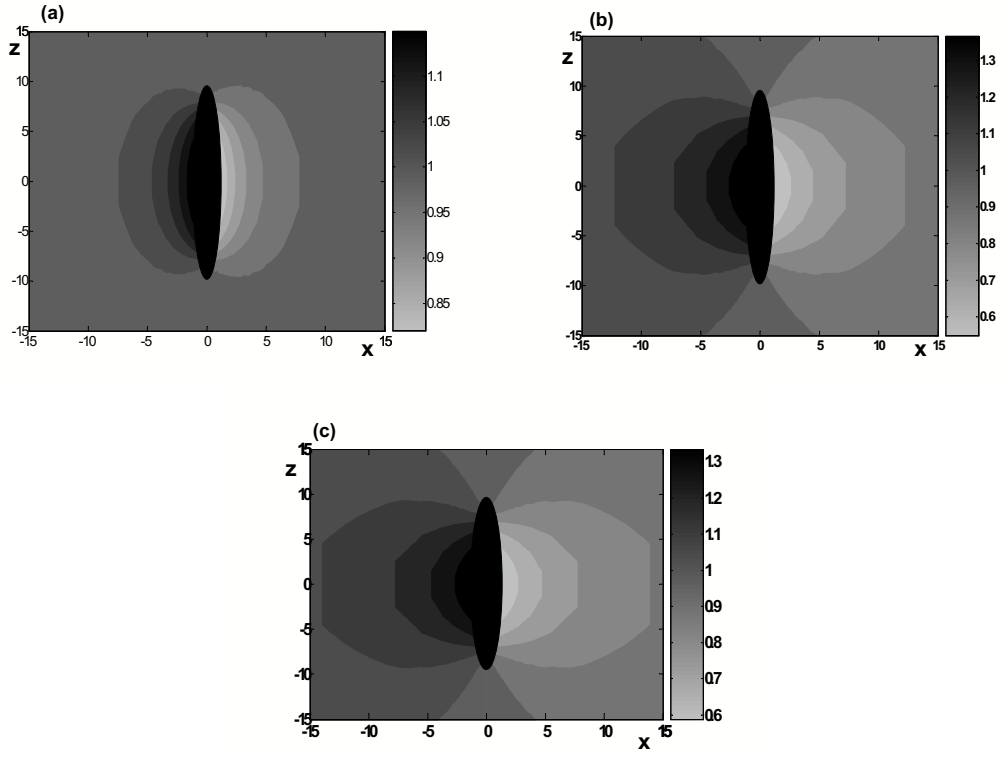

Figure 3: The distribution of the surface tension induced by a stretched obstacle at $Ca = 0.01$, $\theta_0 = 60^\circ$ and (a) $\xi_0^2 = 0.1$, (b) $\xi_0^2 = 10^{-3}$ and (c) $\xi_0^2 = 10^{-4}$. The surface tension is normalised by its value in the far field σ_∞ at $r \to \infty$ and the length is normalised by the slip length λ. The dark black area corresponds to the area occupied by the obstacle.

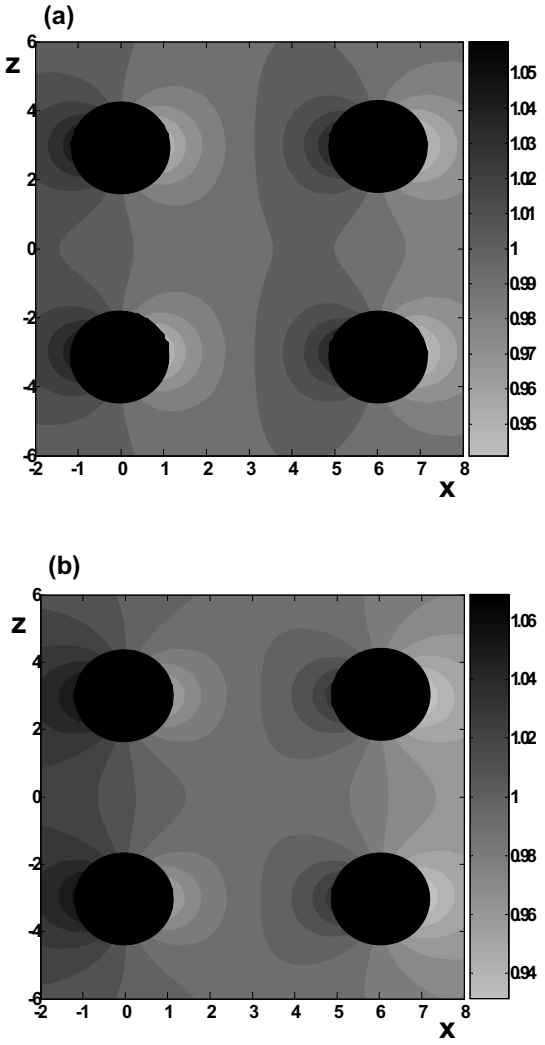

Figure 4: The distribution of the surface tension induced by a group of circular obstacles with $R_0 = 1$ at $Ca = 0.01$, $\theta_0 = 60^\circ$ and (a) $\xi_0^2 = 0.1$, (b) $\xi_0^2 = 10^{-3}$. The surface tension is normalised by its value in the far field σ_∞ at $r \to \infty$ and the length is normalised by the slip length λ. The dark black area corresponds to the area occupied by the obstacles.